Internal report

An Experiment to Definitively Determine the Contributions of Multi-Photon Exchange in Elastic Lepton-Nucleon Scattering

D. Hasell, M. Kohl, R. Milner, V. Ziskin

MIT Laboratory for Nuclear Science and Bates Linear Accelerator Center

J. Arrington

Argonne National Laboratory

December 5, 2006

Abstract

Recent determinations of the proton electric to magnetic form-factor ratio from polarization transfer measurements at Jefferson Lab indicate a significant discrepancy with the form-factor ratio obtained using the Rosenbluth separation technique in unpolarized cross section measurements. This discrepancy has been explained by the effects of multiple photon exchange beyond the usual one-photon exchange approximation in the calculation of the elastic electron-proton scattering cross section. Since most of our understanding on the structure of the proton and atomic nuclei is based upon lepton scattering analyzed in terms of the single photon approximation, it is essential to definitively verify the contribution of multiple photon exchange.

The most direct evidence for multiple photon exchange would be a deviation from unity in the ratio of positron-proton to electron-proton elastic scattering cross sections. In this document, the concept for an experiment to measure this cross section ratio with high precision is developed. Definitive measurements can be carried out in a few months of data taking with a fully operational experiment.

1 Introduction

In the course of the more than 50-year long history of elastic electron-proton scattering since Hofstadter [1] the separation of the proton's electric and magnetic form factors $G_E(Q^2)$ and $G_M(Q^2)$ has been of particular interest. Until the 1990's the experimental method to separate $G_E(Q^2)$ and $G_M(Q^2)$ was based on the procedure by Rosenbluth [2] measuring the unpolarized elastic cross section at fixed four-momentum transfer Q^2 while simultaneously varying the electron scattering angle θ and beam energy. It was found that the Q^2 dependence of both G_E and G_M to a good approximation followed the form of the Fourier transform of an exponentially decaying distribution, namely the dipole form factor $(1+Q^2/0.71)^{-2}$ implying a ratio of $\mu G_E/G_M \approx 1$, shown by the open symbols in Fig. 1 (l.h.s.).

Due to the nature of the Rosenbluth formula

$$\frac{d\sigma/d\Omega}{(d\sigma/d\Omega)_{Mott}} = \frac{G_E^2(Q^2)+\tau G_M^2(Q^2)}{1+\tau} + 2\tau G_M^2(Q^2)\tan^2\frac{\theta}{2} = \frac{\epsilon\, G_E^2(Q^2)+\tau G_M^2(Q^2)}{\epsilon\,(1+\tau)}, \quad (1)$$

where $\tau = Q^2/(4M_p^2)$, the longitudinal virtual photon polarization $\epsilon = [1+2(1+\tau)\tan^2(\theta/2)]^{-1}$, and $(d\sigma/d\Omega)_{Mott} = \alpha/(4E^2)\,(\cos^2\frac{\theta}{2}/\sin^4\frac{\theta}{2})(E'/E)$, the weight of G_E in the cross section becomes less at higher Q^2, making the Rosenbluth separation of $G_E(Q^2)$ and $G_M(Q^2)$ at high momentum transfer rather difficult. While some experiments saw a scaling of the form factors, others occasionally observed significant deviations of the ratio $\mu G_E/G_M$ from unity. The world data collection on elastic e-p scattering has recently been compiled by [3]. The most recent Rosenbluth-type measurements have again confirmed the scaling behavior of the proton form-factor ratio [4, 5], and additional unpolarized precision measurements are planned [6].

In the late 1990's, development of polarized beams, targets and polarimeters allowed a new way to measure the form-factor ratio more directly through the interference of G_E and G_M in the spin-dependent elastic cross section asymmetry [7, 8, 9, 10]. It came as a big surprise when the high precision polarization transfer measurements at Jefferson Laboratory at higher Q^2 up to 5.5 (GeV/c)^2 gave striking evidence that the proton form-factor ratio $\mu G_E/G_M$ is monotonically falling with Q^2 [11, 12, 13]. This Q^2 dependence was dramatically different from that observed with the unpolarized Rosenbluth method. Linear extrapolation of G_E would even suggest a node of the electric form factor near 8 (GeV/c)^2. Note that this decline of the proton form-factor ratio was predicted already in 1973 by calculations based on vector-meson dominance, including the expected node around 8 (GeV/c)^2 [19], as shown in Fig. 1 (r.h.s.). Future recoil polarization experiments at Jefferson Lab will extend the Q^2 range up to 9 (GeV/c)^2 with a new recoil polarimeter [14] and up to 14 (GeV/c)^2 after the 12-GeV upgrade [15].

Alternative measurements of G_E/G_M are based on the spin-dependent asymmetries with polarized beam and target. Experiments of this kind are considered equivalent to polarization transfer and constitute important independent tests to verify the recoil polarization results. Such measurements have recently been performed with the Bates Large Acceptance Spectrometer Toroid (BLAST) at low Q^2 using an internal polarized hydrogen target [16]. The result is consistent with scaling of the form factor ratio, albeit at low Q^2 where no discrepancy between polarized and unpolarized measurements was expected. Another experiment used a frozen-spin ammonia target [17] to extract the form-factor ratio at somewhat higher $Q^2 \approx 1.51$ (GeV/c)^2, with a result for $\mu G_E/G_M$ between the unpolarized and polarization transfer data (solid circle in left plot of Fig. 1). Clearly, further measurements are needed to resolve this discrepancy.

2 Beyond the Single Photon Approximation

The generally accepted explanation for the discrepancy between the recoil polarization and Rosenbluth determinations of the elastic proton form factor ratio is the exchange of multiple (>1) photons during the electron-proton elastic scattering process [20, 21].

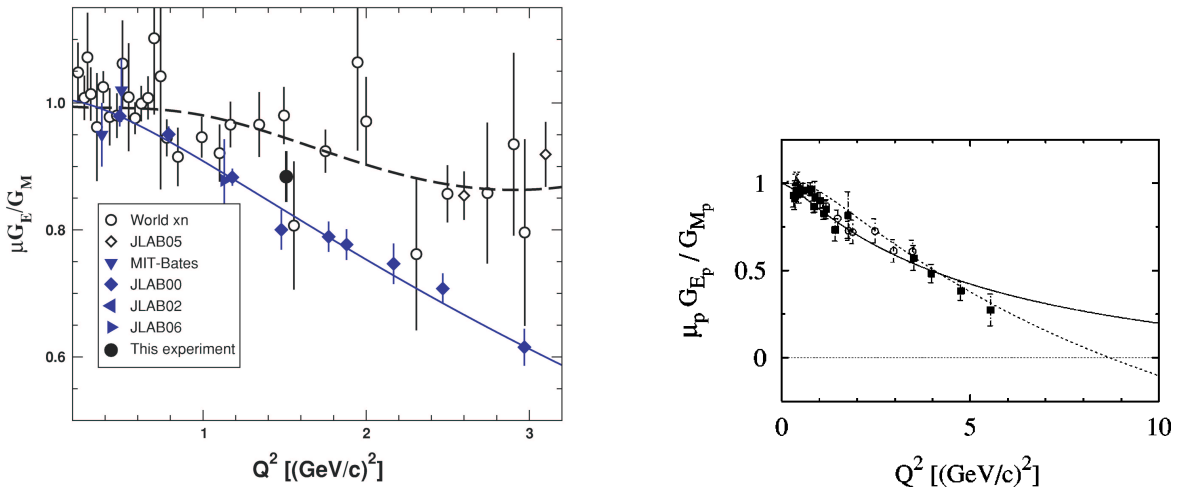

Figure 1: L.h.s.: Proton electric to magnetic form-factor ratio $\mu G_E/G_M$ from unpolarized (open symbols, "World xn" and JLAB05 [3, 5]) and polarized measurements (filled symbols, MIT-Bates [7], JLAB00 [11], JLAB02 [12], and JLAB06 [13]). The figure has been taken from [17] ("this experiment"). The curves are fits to unpolarized data [3] and to data from [11, 12] only for the high-Q^2 region. R.h.s.: Form-factor ratio $\mu G_E/G_M$ from recoil polarization compared with calculations by Iachello from 2004 (solid) [18] and 1973 (dashed) [19].

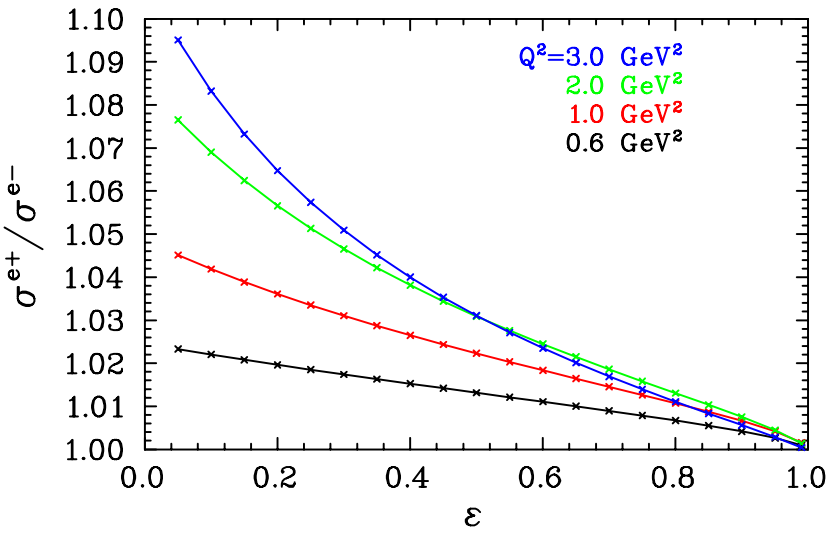

Figure 2: Ratio of elastic positron-proton to electron-proton cross section versus virtual photon polarization for given Q^2 [21].

This implies that certain lepton-nucleon scattering observables will differ significantly from their one-photon exchange (or first-order Born approximation) expectation value.

Multiple-photon exchange processes will exhibit a characteristic dependence of the elastic lepton-proton scattering cross section on the value of virtual photon polarization ϵ. As ϵ decreases, the effects of multiple-photon exchange on the elastic cross section tend to increase in magnitude.

The discrepancy between the recoil polarization and Rosenbluth determinations of the elastic proton form-factor ratio grows with increasing Q^2. At high Q^2, the cross section is dominated by magnetic (i.e. transverse) scattering. This explains why the effect on the extraction of G_E from Rosenbluth separations can be sizable, while the effect on the cross section at all values of Q^2 is rather modest. At the same time, the form-factor ratio from polarization experiments is less affected.

The effect of multiple-photon exchange on the electromagnetic elastic form factors involves the real part of the multiple-photon exchange amplitude. The observable most sensitive to this amplitude is the ratio of the elastic cross section for electron-proton to positron-proton scattering. In the presence of multiple-photon exchange, the cross section for unpolarized lepton-proton scattering contains an interference term between the one- and two-photon amplitudes. This interference is odd under time reversal, and hence has the opposite sign for elastic positron-proton and electron-proton scattering, respectively. Therefore, a non-zero two-photon amplitude would result in different cross sections for unpolarized electron-proton and positron-proton scattering.

Figure 2 shows the ratio of the two cross sections as a function of the virtual photon

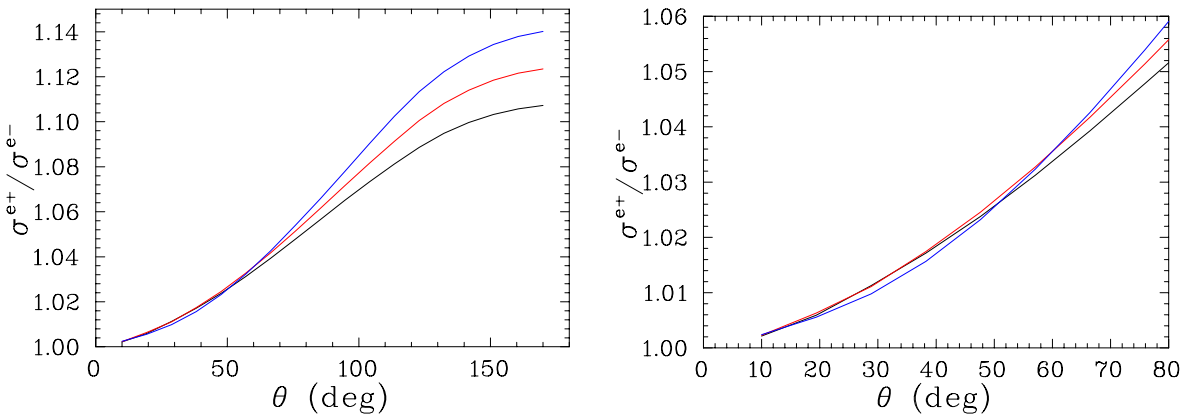

Figure 3: e^+p/e^-p cross section ratio as a function of scattering angle, for three beam energies (black=2.0 GeV, red=2.5 GeV, blue=3.0 GeV) [21]. The figure on the right shows the region up to 80° where only little energy dependence of the two-photon effect is evident.

polarization ϵ. The ratio would be unity in the case of pure single photon exchange, i.e. the Born approximation. The sensitivity is enhanced at low ϵ, exceeding 4% for $\epsilon \leq 0.4$, provided $Q^2 \geq 2$ (GeV/c)^2. Beyond $Q^2 = 2$ (GeV/c)^2 the Q^2 dependence of the two-photon effect is small, and since the cross section decreases rapidly with Q^2, one would want to keep Q^2 as low as possible for optimized statistics. This is clear in Fig. 3 which displays the e^+p/e^-p cross section ratio as a function of the scattering angle for three beam energies. Up to about 80°, the cross section ratio is almost independent of the beam energy, and hence of Q^2 for a given scattering angle.

Figure 4 shows the elastic proton electric to magnetic form factor ratio under various conditions: The red diamonds correspond to the form-factor ratio as determined from recoil polarization, which has only little sensitivity to multi-photon effects. The magenta crosses correspond to the form-factor ratio from existing e^-p Rosenbluth separation data (Bosted fit [22]). The green open circles represent the effect of two-photon exchange on the Rosenbluth measurements, using a simple fit to the two-photon correction that explains that discrepancy between polarization and Rosenbluth measurements. The blue solid circles are the result of applying this two-photon correction to Rosenbluth measurements using e^+p scattering. The expected node at ≈ 2.6 (GeV/c)^2 is remarkable. Above 2.6 (GeV/c)^2, one would expect to find negative values for $G_E^{p\,2}$ from e^+-p Rosenbluth separations.

Previous experiments from the 1960's at SLAC [23] have measured the e^+p / e^-p cross section ratio. However, high-precision measurements with uncertainties of 1% were done only at low Q^2 or very large ϵ, where the multiple-photon exchange effects appear to be small. Measurements at low ϵ had uncertainties of $\approx 5\%$, too large to see conclusive deviations from unity. Recent reanalysis of the (limited) low-ϵ data give an

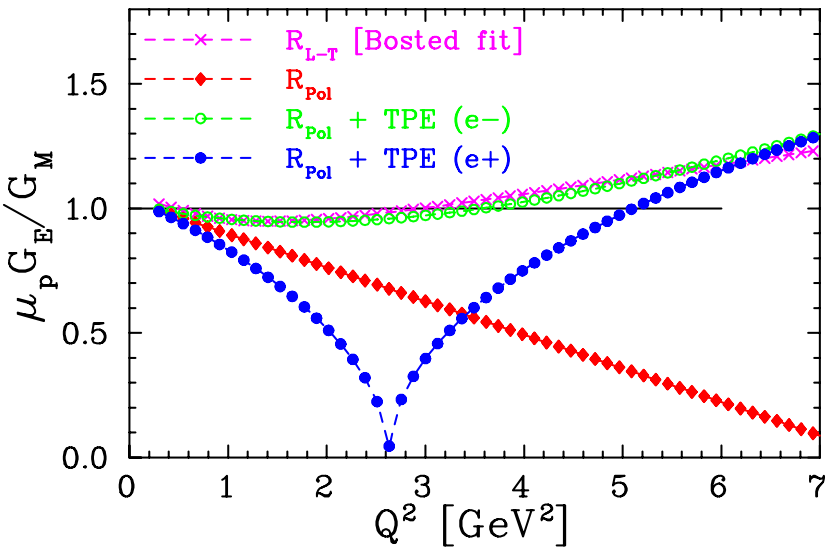

Figure 4: Proton electric to magnetic form-factor ratio $\mu_p G_E^p/G_M^p$ without (red diamonds) and with two-photon effects calculated for e^--p (green open circles) and e^+-p (blue solid circles) Rosenbluth separations [21]. The magenta crosses represent a fit to existing Rosenbluth-separated e^--p data. The electric form factor G_E^p from unpolarized e^+-p scattering has a node expected at $Q^2 \approx 2.6$ (GeV/c)^2, with ${G_E^p}^2 < 0$ for $Q^2 > 2.6$ GeV/c)^2.

indication of multiple-photon exchange effects, consistent with recent calculations, but only at the three-sigma level [3].

Recently, two new experiments have been proposed to study the e^+p and e^-p cross section ratio: one at Jefferson Lab [24] using a secondary electron/positron beam from a pair production target, and another at Novosibirsk [25] based on stored electron and positron beams incident on an internal unpolarized hydrogen target.

The effect of two-photon exchange on the real part of the lepton-nucleon scattering amplitude can also be investigated by studying the ϵ-dependence of the proton form-factor ratio from polarization experiments. Such an experiment has been proposed at Jefferson Lab [26]. Precise mapping of Rosenbluth cross sections in unpolarized e^-p scattering will also reveal any nonlinearities in the ϵ dependence of the cross section [6].

The imaginary part of the two-photon amplitude would give rise to non-zero transverse single-spin asymmetries, of either the beam (A_n), the target (A_y) or the induced polarization (P_y). These single-spin asymmetries will be studied at Jefferson Lab as well [26, 27].

In this document, we argue that the use of the intense, multi-GeV stored electron and positron beams at the storage ring DORIS at DESY, Hamburg, Germany in combination with the BLAST detector can produce the most definitive data to determine the

effect of multiple photon exchange in elastic lepton-proton scattering and verify the recent theoretical predictions.

3 Proposed Experiment

We propose to measure the ratio of elastic electron-proton to positron-proton cross sections over a range of ϵ with the BLAST detector using an internal unpolarized hydrogen target and intense stored beams of unpolarized positrons and electrons at energies between 2.3 and 4.5 GeV at the storage ring DORIS at DESY in Hamburg, Germany. To carry out this experiment will require

- operation of the DORIS storage ring at different energies and with both electrons and positrons
- the relocation of the BLAST detector from MIT-Bates to DESY/DORIS and
- the installation of an unpolarized hydrogen internal gas target.

At DORIS, both electron and positron beams can be stored with high intensity and energies up to 4.5 GeV. The DORIS storage ring was operated as a e^+-e^- collider until 1993, and is is currently used as a source for synchrotron radiation using 100 mA positrons with a lifetime of about 20 hours. Before 1993, beam intensities for electrons were on the order 50 mA, but currents on the order of 100 mA should now be possible.

With sufficient luminosity and appropriate control of systematic uncertainties, a storage ring experiment with both electrons and positrons incident on an internal hydrogen gas target is the best way to measure the e^+p/e^-p cross section ratio. Simultaneous measurement both at low and at high ϵ with a large-acceptance detector configuration (BLAST) will allow a determination of the ϵ-dependence of the cross section ratio, and hence the size of the two-photon amplitude. Measurement at different beam energies will also enable a Rosenbluth separation for the positron cross sections for a wide range of four-momentum transfer when the measured e^+p/e^-p ratios are combined with existing Rosenbluth data for elastic electron-proton scattering.

3.1 Detector

We propose to utilize the existing Bates Large Acceptance Spectrometer Toroid (BLAST) detector system from MIT-Bates. BLAST is a toroidal spectrometer with eight sectors. The two in-plane sectors are instrumented with wire chambers for

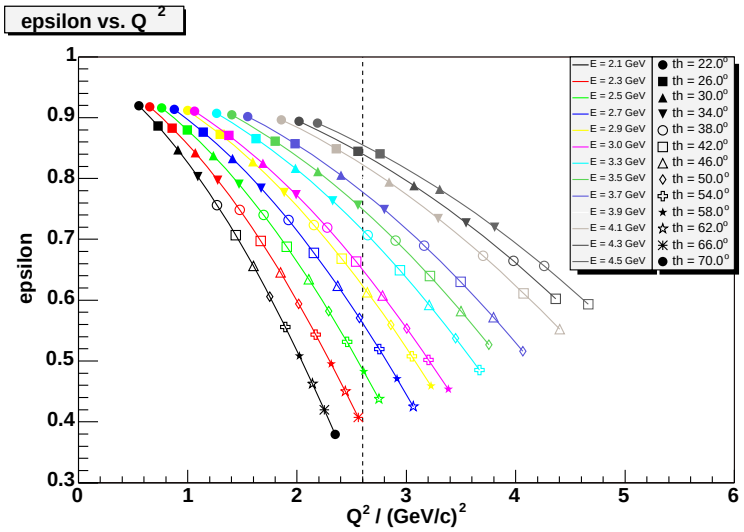

Figure 5: Kinematic coverage of ϵ versus Q^2 for the BLAST detector for various beam energies.

charged-particle tracking, plastic scintillators for trigger and particle identification, and aerogel-Cerenkov counters for pion rejection. The detector is symmetric about the beam direction and allows for complete reconstruction of coincident elastic events with both electron and proton four-vectors being determined. The symmetry of the detector doubles the solid angle for elastic scattering. The angle acceptance covers approximately 20° to 80° of the polar and ±15° of the azimuthal angle.

In order to demonstrate the kinematic coverage of the BLAST detector, Fig. 5 shows the virtual photon polarization ϵ versus Q^2 for different beam energies (colors) and different scattering angles (symbols), with each set of symbols corresponding to the acceptance of BLAST. For any beam energy given, the parameters ϵ and Q^2 are kinematically correlated within the large angle acceptance. For the BLAST detector geometry, the acceptance becomes smaller at higher beam energies, thereby setting a lower limit for the reachable value of ϵ, since for backward lepton scattering angles the scattered proton is recoiling at decreasing angles and eventually misses the detector system. For the acceptance limitation by BLAST a proton angle $\theta_p > 23°$ was assumed.

As a consequence, the lowest reachable values of ϵ are about 0.4 and are only established at a beam energy of less than 2.3 GeV. At the same time, the beam energy should also not be smaller than 2 GeV in order to maintain a high enough $Q^2 > 2$ (GeV/c)^2.

For a fixed Q^2 of 2.6 (GeV/c)^2 (where the $G_E(e^+)$ node is expected), only beam energies of 2.3-4.5 GeV are appropriate for use with BLAST. At this value of Q^2 the BLAST acceptances for these beam energies are overlapping, suitable to map out the ϵ dependence of the cross section ratio at fixed Q^2 (similar to a Rosenbluth separation).

The lowest beam energy corresponds to the lowest ϵ value for that respective Q^2 value. In combination with existing electron-proton cross sections, a Rosenbluth separation of the positron-proton elastic cross section can be carried out.

3.2 Target

The target will be an unpolarized hydrogen source connected directly to a thin walled, cryogenically cooled aluminum tube, similar to that used in the HERMES/DESY and BLAST/MIT experiments. To carry out measurements of the elastic electron-proton cross section at the lowest value of $\epsilon \approx 0.4$ with $\approx 1\%$ statistical uncertainty in about 1 month, a luminosity of $6 \cdot 10^{32}/(\mathrm{cm}^2\mathrm{s})$ will be required for this experiment. Assuming 100 mA circulating electron and positron currents, this implies a target thickness of about 10^{15} atoms/cm^2. Large vacuum pumps will be required to pump away the hydrogen gas so that the lifetime of the stored beam can be on the order of several hours. The Argonne and MIT groups have considerable experience in designing, installing and operating such internal gas targets in storage rings [28].

We can estimate the beam lifetime in DORIS based on a simple model for losses accounting for bremsstrahlung, Moller and Rutherford scattering [29]. The current aperture at DORIS is limited by an undulator with an 11mm gap, allowing only for a vertical emittance of about 7 mm mrad. The momentum acceptance of DORIS (or bucket size) is estimated with 0.8%. The lifetime without any target in the current operation mode as a lightsource is on the order of 20 h. Figure 6 shows the expected partial lifetimes due to the various above mentioned processes that are causing losses, along with the resulting lifetime. It is assumed that the insertion of a target cell does not further limit the aperture. With a beta function sufficiently small at the location of the target, which can be achieved with a set of quadrupole magnets upstream and downstream of the internal target, this is a realistic assumption. The expected lifetime at a beam energy of 2.3 GeV amounts to 10.6 h for a target thickness of 10^{14} atoms/cm^2 and 2.0 h for the required thickness of 10^{15} atoms/cm^2. The momentum acceptance is still the dominant limitation. In comparison, the lifetime at MIT-Bates with a target thickness of $5 \cdot 10^{13}$ atoms/cm^2 was about 30 minutes.

If DORIS can be operated in top-up mode, the consideration on the ring lifetime may be even less important.

3.3 Luminosity Monitor

The target thickness will be monitored over time by continuously measuring the pressure and temperature of the reservoir and by an additional flow meter to measure the

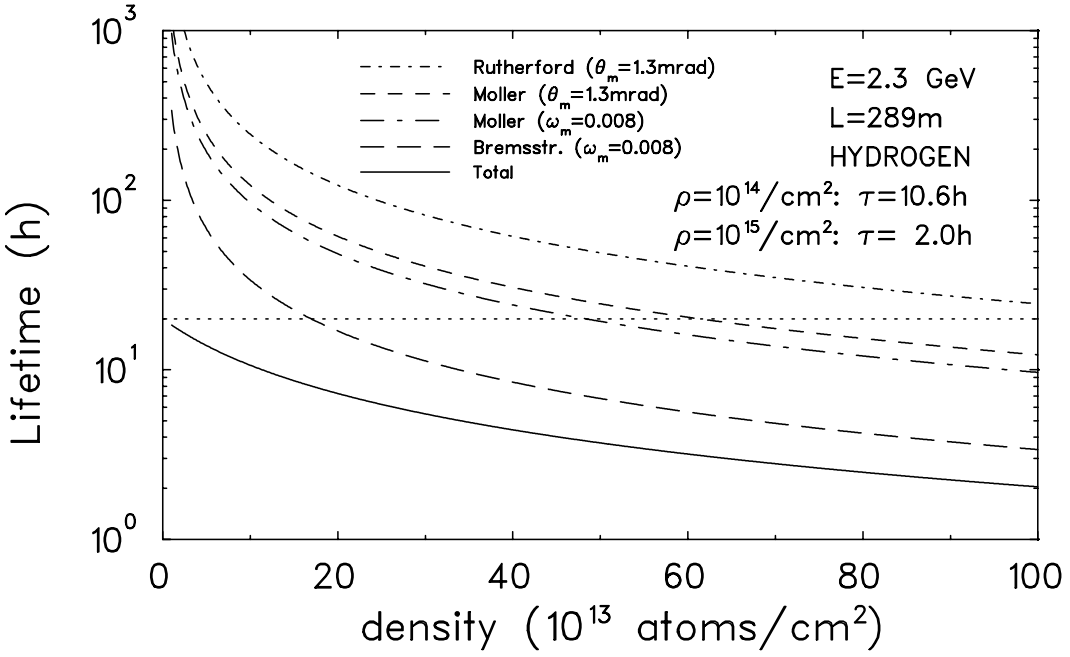

Figure 6: Expected beam lifetime in DORIS as a function of the target thickness. Based on a lifetime of 20h without target (dotted line), the lifetime is reduced by Rutherford and Moller scattering and bremsstrahlung due to the given aperture limits (angle acceptance θ_m and momentum accptance ω_m).

flux from the buffer. The stored current of positrons and electrons in the ring will be measured with an absolute precision of 1% with a parametric current transformer as was done for BLAST running at MIT-Bates, providing a precise monitor of the luminosity when combined with the gas flow information from the buffer system.

Besides measuring target thickness and beam current explicitly, we also propose to measure and monitor the luminosity with elastic scattering at low momentum transfer. At low $Q^2 < 1$ (GeV/c)^2, the proton form factors G_E and G_M are well known at the 1% level. Moreover, at ϵ close to 1, two-photon effects are expected to be negligible, hence the rate for both e^+-p and e^-p elastic scattering is proportional to the luminosity.

E_0 [GeV]	Q^2 [(GeV/c)^2]	$p_{e'}$ [GeV/c]	ϵ	θ_p	p_p [MeV/c]	Rate [h^{-1}]
4.5	0.574	4.194	0.9825	63.1°	816	37616
3.0	0.262	2.860	0.9837	69.8°	530	196601
2.3	0.154	2.217	0.9844	73.2°	400	467075

Table 1: Kinematics and count rates of the luminosity control measurement for three beam energies at $\theta_e = 10°$. The assumed solid angle is 22.5 msr.

To this extent, we will use a position-sensitive counter at a forward angle of about 10° to detect electrons or positrons in coincidence with the recoiling proton at large angle covered by the acceptance of BLAST. At such a forward angle, the field integral of the BLAST toroid is quite small, resulting in almost straight tracks for elastically scattered electrons and positrons. The forward-angle detector will have to be radiation-hard, capable of handling high rates in the MHz region and has to provide good angular ($< 0.5°$) and vertex resolution (< 1 cm) for the forward tracks.

One possibility for the forward detector would be a package of two 30×30 cm^2 planar triple-GEM detectors, identical to the COMPASS-GEM [30], allowing to measure the lepton tracks with high resolution. An alternative option would be several crossed layers of thin scintillator hodoscopes read out on both ends with fast photomultipliers for good position resolution. We will also use a Cerenkov counter or electromagnetic shower calorimeter behind the position-sensitive element to identify the electrons and positrons. At a distance of 200 cm from the target, a solid angle of 22.5 msr is covered by the area of 30×30 cm^2. The angular resolution of the track should be better than 0.5°, which corresponds to a spatial resolution requirement of 1.7 cm. While this modest requirement can already be achieved with the hodoscope, a higher resolution may be required if also the vertex needs to be resolved. The final decision will be based on a more detailed study.

For beam energies between 2.3 and 4.5 GeV, the four-momentum transfer at $\theta_e = 10°$ varies beween 0.15 and 0.57 (GeV/c)^2, and the virtual photon polarization parameter ϵ is above 0.98. Here the single photon approximation is good to better than 1%. The proton is recoiling with momenta of 400-800 MeV/c at angles of 63°-73°, well within the rear-angle acceptance of the BLAST detector.

The coincidence requirement between the forward detector and BLAST as well as further kinematic correlations between the lepton and proton track will suppress backgrounds from any source including random coincidences.

The cross section at low Q^2 and $\epsilon > 0.98$ is large enough to provide $< 1\%$ statistical error for the above configuration in less than one hour, indicating the suitability of this setup as a luminosity monitor. The expected count rate for this luminosity monitor is listed for three beam energies in Tab. 1.

E_0 [GeV]	Q^2 [(GeV/c)^2]	θ_e	$p_{e'}$ [GeV/c]	ϵ	θ_p	p_p [GeV/c]
4.5	2.6	24.9°	3.114	0.86	38.0°	2.125
3.0	2.6	43.0°	1.614	0.65	31.2°	2.125
2.3	2.6	67.6°	0.914	0.39	23.4°	2.125

Table 2: Kinematics for three beam energies and $Q^2 = 2.6$ (GeV/c)^2.

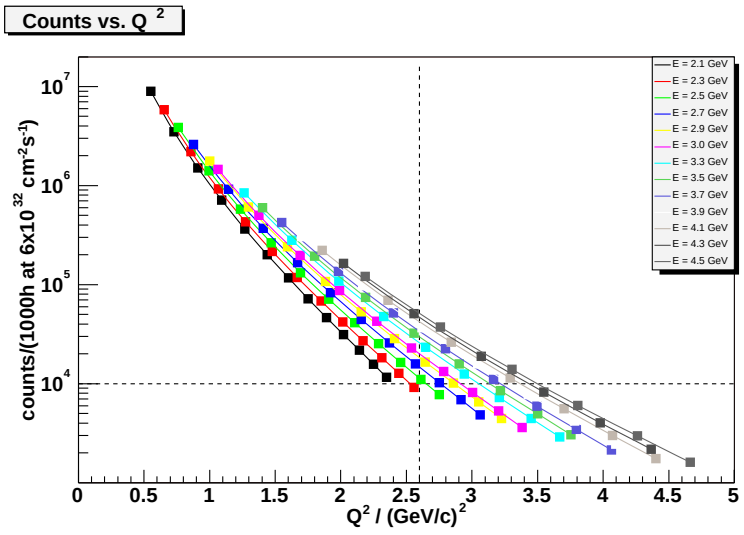

Figure 7: Expected distribution of counts per marked angle bin for the BLAST detector for various beam energies, as a function of Q^2. The assumed luminosity is $6{\cdot}10^{32}/(\mathrm{cm}^2\mathrm{s})$ $\times$ 1000 hours.

3.4 Count Rate Estimate

Figure 7 shows the expected number of counts in any given angle bin and for various beam energies for a canonical run of 1000h at a luminosity of $6{\cdot}10^{32}/(\mathrm{cm}^2\mathrm{s})$ as a function of Q^2. Höhler form factor [31] based cross sections where used for this estimate, good enough within 10% for both e^+ and e^- up to $Q^2 \approx 3$ $(\mathrm{GeV/c})^2$. We see that for $Q^2 = 2.6$ $(\mathrm{GeV/c})^2$, the number of counts per angle bin ranges between $\approx 10^4$ (at 2.1 $(\mathrm{GeV/c})^2$ and smallest ϵ and $\approx 7 \cdot 10^4$ (at 4.5 $(\mathrm{GeV/c})^2$ and highest ϵ).

The next plot in Fig. 8 shows the expected number of counts in any given angle bin and for various beam energies versus ϵ. Generally, lowest ϵ values at reasonable counts of $> 10^4$ are possible down to $\epsilon \approx 0.4$, for which the beam energy should not exceed 2.3 GeV. At higher energies, the lowest value of ϵ reachable with the rearmost scattering angle increases, while at the same time the count rate decreases.

Measurements at three beam energies, as listed in Tab. 2, will yield precise ratios of e^+-p and e^--p cross sections at $Q^2 = 2.6$ $(\mathrm{GeV/c})^2$ for a wide range of ϵ. The counts for each Q-point in the table are in excess of $\approx 10^4$ counts. In combination with world electron-proton cross section data this allows for a precise Rosenbluth separation of the elastic positron-proton cross section.

At $\epsilon = 0.4$ and $Q^2 = 2.6$ $(\mathrm{GeV/c})^2$, the effect on $\sigma(e^+/e^-)$ is expected to be of the order 4%. For a 1% statistical error of the cross section ratio, about $2 \cdot 10^4$ counts are required for both electron and positron measurements. For the sum of the three lowest

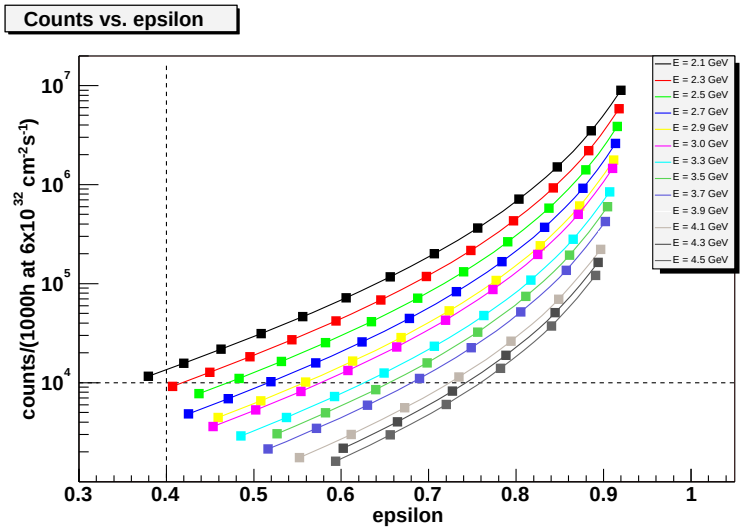

Figure 8: Expected distribution of counts per marked angle bin for the BLAST detector for various beam energies, as a function of ϵ. The assumed luminosity is $6 \cdot 10^{32}/(\mathrm{cm}^2\mathrm{s})$ $\times$ 1000 hours.

ϵ bins $\theta_e = 58°, 62°$, and $66°$ at 2.3 GeV in Tab. 3, each electron and positron cross section measurement takes about 500h under the conditions discussed above.

It should be emphasized that the large angular acceptance of BLAST includes a wide distribution of ϵ values in a single measurement. Table 3 summarizes kinematics and expected count rate per angle bin for the three beam energies.

3.5 Control of Systematics

The primary observable of this experiment is the *ratio* of the electron-proton and positron-proton elastic cross sections. The redundant control measurements of the luminosity will allow to determine the e^+-p/e^-p cross section ratio with high precision. As is shown below, the systematic errors for individual proton and lepton acceptance and efficiency will cancel to first order.

In order to reduce the systematic errors of the cross section ratio due to uncertainties in relative luminosity, acceptance and efficiency with individual electron and positron beams, we require that the beam storage in DORIS will often be alternated between electrons and positrons, and that the BLAST magnet polarity be reversed with the same frequency. With the same polarity of the BLAST magnet, the acceptance and efficieny for the recoiling protons κ^p will be identical, however the electron and positron acceptance and efficiency κ^l may differ from each other. When reversing the BLAST

E_0 [GeV]	θ_e	$p_{e'}$ [GeV/c]	θ_p	p_p [GeV/c]	Q^2 [(GeV/c)^2]	ϵ	Counts
4.5	**22**	**3.33**	**41.6**	**4.17**	**2.2**	**0.891**	**121357**
	26	**3.03**	**36.8**	**3.85**	**2.8**	**0.840**	**37382**
	30	**2.74**	**32.8**	**3.56**	**3.3**	**0.782**	**13924**
	34	**2.47**	**29.4**	**3.28**	**3.8**	**0.720**	**6046**
	38	**2.23**	**26.6**	**3.03**	**4.3**	**0.656**	**2971**
	42	**2.01**	**24.2**	**2.80**	**4.7**	**0.593**	**1614**
							183294
3.0	**22**	**2.43**	**50.8**	**3.24**	**1.1**	**0.910**	**1463770**
	26	**2.27**	**45.9**	**3.06**	**1.4**	**0.871**	**500148**
	30	**2.10**	**41.6**	**2.89**	**1.7**	**0.825**	**196674**
	34	**1.94**	**37.9**	**2.72**	**2.0**	**0.774**	**87256**
	38	**1.79**	**34.7**	**2.56**	**2.3**	**0.719**	**42907**
	42	**1.65**	**31.8**	**2.41**	**2.5**	**0.663**	**23025**
	46	**1.52**	**29.3**	**2.27**	**2.8**	**0.608**	**13304**
	50	**1.40**	**27.1**	**2.14**	**3.0**	**0.554**	**8183**
	54	**1.29**	**25.1**	**2.02**	**3.2**	**0.502**	**5306**
	58	**1.20**	**23.3**	**1.92**	**3.4**	**0.454**	**3599**
							2344172
2.3	**22**	**1.95**	**56.1**	**2.73**	**0.7**	**0.918**	**5842290**
	26	**1.84**	**51.5**	**2.62**	**0.9**	**0.883**	**2203890**
	30	**1.73**	**47.2**	**2.50**	**1.1**	**0.842**	**927333**
	34	**1.62**	**43.5**	**2.38**	**1.3**	**0.797**	**429793**
	38	**1.51**	**40.1**	**2.26**	**1.5**	**0.748**	**216921**
	42	**1.41**	**37.1**	**2.15**	**1.7**	**0.697**	**117977**
	46	**1.31**	**34.3**	**2.05**	**1.8**	**0.645**	**68486**
	50	**1.23**	**31.9**	**1.95**	**2.0**	**0.594**	**42073**
	54	**1.14**	**29.6**	**1.86**	**2.2**	**0.544**	**27146**
	58	**1.07**	**27.6**	**1.77**	**2.3**	**0.496**	**18276**
	62	**1.00**	**25.8**	**1.69**	**2.4**	**0.450**	**12765**
	66	**0.94**	**24.1**	**1.62**	**2.6**	**0.407**	**9204**
							9916154

Table 3: Kinematics for three beam energies and count estimate per 4°-angle bin for 1000h at $6 \cdot 10^{32}$ / (cm^{2}s). For the higher beam energy the backward lepton angle acceptance is limited by the forward proton angle.

magnetic field, the positron acceptance in one polarity will equal the electron acceptance with reversed polarity of BLAST. In this case however, the proton acceptance and efficiency may be different for each polarity. The same consideration holds for the events measured with the forward-angle luminosity monitor.

Frequent and random filling with both e^+ and e^- beams and reversal of the BLAST field direction will minimize systematic uncertainties in the ratio from acceptance and efficiency differences as statistics are accumulated. For a given bin, the number of events $N_{ij} = L_{ij}\sigma_i\kappa^p_{ij}\kappa^l_{ij}$ will be recorded for the four combinations ij, where $i = e^+(e^-)$ for positrons (electrons) and $j = +(-)$ for positive (negative) BLAST polarity, where L is the luminosity and σ the bin-averaged lepton-nucleon cross section.

For a given polarity j, the proton efficiencies κ^p_{ij} cancel in the ratio

$$\frac{N_{e^+j}/L_{e^+j}}{N_{e^-j}/L_{e^-j}} = \frac{\sigma_{e^+}}{\sigma_{e^-}} \cdot \frac{\kappa^l_{e^+j}}{\kappa^l_{e^-j}} \tag{2}$$

due to $\kappa^p_{e^+j} = \kappa^p_{e^-j}$. With the above cancellations of $\kappa^l_{e^++} = \kappa^l_{e^--}$ and $\kappa^l_{e^+-} = \kappa^l_{e^-+}$, the combination

$$\left[\frac{N_{e^++}/L_{e^++}}{N_{e^-+}/L_{e^-+}} \cdot \frac{N_{e^+-}/L_{e^+-}}{N_{e^--}/L_{e^--}}\right]^{\frac{1}{2}} = \frac{\sigma_{e^+}}{\sigma_{e^-}} \tag{3}$$

measures the cross section ratio directly where all lepton and proton acceptances and efficiencies cancel to first order for a cycle of four combinations. The same consideration holds for the combination of the four luminosities L_{ij} which only occur in ratios where the respective geometrical efficiencies cancel. The cycle will then be repeated for the appropriate number of times. The cycle has to be short enough to ensure the cancellations of efficiencies, which are slowly varying quantities. It appears appropriate that every combination takes one day of running, i.e. every other day the beam and the polarity, respectively, will be switched in a staggered way.

The left-right symmetry of the BLAST detector is another feature that will be used to control systematic uncertainties: As the unpolarized cross section is independent of the azimuthal angle, the production rate in both sector combinations are expected to be equal, and their difference is a measure how well the cancellations of the relative efficiency work.

The above scheme makes use of measurements of the proton and lepton tracks in coincidence. Further information and additional checks of systematics will be obtained from proton or lepton single-arm events for which the high and low ϵ limits of the BLAST acceptance are extended. Provided that backgrounds in single-arm elastic events can be kept at a minimum, proton single-arm ratios for electron and positron beams with the same polarity of BLAST, as well as lepton single-arm ratios with reversed field polarity also probe the e^+/e^- cross section ratio independently.

4 Conclusion

The current discrepancy between recoil polarization and Rosenbluth measurements of the proton elastic form-factor ratio constitutes a serious challenge which undermines our understanding of the structure of the proton. The widely accepted explanation in terms of multiple photon exchange demands a definitive confirmation.

A precision study of the e^+-p/e^--p cross section ratio will directly test the contribution of multiple photon effects. As the prediction of the magnitude of multiple photon effect is model-dependent, the experiment described here will provide a strong constraint to theoretical calculations.

The proposed experiment we describe here takes advantage of unique features of the BLAST detector combined with an internal hydrogen gas target in a storage ring for electrons and positrons. The systematic uncertainties are controllable at the percent level, and with the superior luminosity that can be provided at DORIS, this experiment will not be limited in statistical precision.

References

[1] R. Hofstadter, Rev. Mod. Phys. **28**, 214 (1956).

[2] M.N. Rosenbluth, Phys. Rev. **79**, 615 (1950).

[3] J. Arrington, Phys. Rev. **C69**, 022201(R) (2004).

[4] M.E. Christy *et al.*, Phys. Rev. **C70**, 015206 (2004).

[5] I.A. Qattan *et al.*, Phys. Rev. Lett. **94**, 142301 (2005).

[6] J. Arrington *et al.*, *A measurement of two-photon exchange in unpolarized elastic electron-proton scattering*, Jefferson Lab Proposal E05-017 (2005).

[7] B. Milbrath *et al.*, Phys. Rev. Lett. **80**, 452 (1998); Erratun-ibid. Phys. Rev. Lett. **82**, 2221(E) (1999).

[8] S. Dieterich *et al.*, Phys. Lett. **B500**, 47 (2001).

[9] T. Pospischil *et al.*, Eur. Phys. J. **A12**, 125 (2001).

[10] O. Gayou *et al.*, Phys. Rev. **C64**, 038202 (2001).

[11] V. Punjabi *et al.*, Phys. Rev. **C71**, 055202 (2005); Erratum-ibid. Phys. Rev. **C71**, 069902(E) (2005); M. Jones *et al.*, Phys. Rev. Lett. **84**, 1398 (2000).

[12] O. Gayou *et al.*, Phys. Rev. Lett. **88**, 092301 (2002).

[13] G. MacLachlan *et al.*, Nucl. Phys. **A764**, 261 (2006).

[14] C. Perdrisat *et al.*, Jefferson Lab Proposals E01-109, E04-108.

[15] J. Arrington *et al.*, Conceptual Design Report CD0, Hall C 12 GeV Upgrade (2002).

[16] C. Crawford, A. Sindile, T. Akdogan, R. Alarcon, W. Bertozzi, E. Booth, T. Botto, J. Calarco, B. Clasie, A. DeGrush, T.W. Donnelly, K. Dow, D. Dutta, M. Farkhondeh, R. Fatemi, O. Filoti, W. Franklin, H. Gao, E. Geis, S. Gilad, W. Haeberli, D. Hasell, W. Hersman, M. Holtrop, P. Karpius, M. Kohl, H. Kolster, T. Lee, A. Maschinot, J. Matthews, K. McIlhany, N. Meitanis, R.G. Milner, J. Rapaport, R.P. Redwine, J. Seely, A. Shinozaki, S. Širca, E. Six, T. Smith, B. Tonguc, C. Tschalaer, E. Tsentalovich, W. Turchinetz, J.F.J. van den Brand, J. van der Laan, F. Wang, T. Wise, Y. Xiao, W. Xu, C. Zhang, Z. Zhou, V. Ziskin, and T. Zwart, submitted to Phys. Rev. Lett.;
C. Crawford, Ph.D. thesis, MIT (2005);
A. Sindile, Ph.D. thesis, University of New Hampshire (2006).

[17] M.K. Jones *et al.*, Phys. Rev. **C74**, 035201 (2006).

[18] R. Bijker and F. Iachello, Phys. Rev. **C69**, 068201 (2004).

[19] F. Iachello, A.D. Jackson, and A. Lande, Phys. Lett. **B43**, 191 (1973).

[20] P.A.M. Guichon and M. Vanderhaeghen, Phys. Rev. Lett. **91**, 142303 (2003); P.G. Blunden, W. Melnitchouk, and J.A. Tjon, Phys. Rev. Lett. **91**, 142304 (2003); M.P. Rekalo and E. Tomasi-Gustafsson, Eur. Phys. J. **A22**, 331 (2004); Y.C. Chen, A.V. Afanasev, S.J. Brodsky, C.E. Carlson and M. Vanderhaeghen, Phys. Rev. Lett. **93**, 122301 (2004); A.V. Afanasev and N.P. Merenkov, Phys. Rev. D **70**, 073002 (2004).

[21] P.G. Blunden, W. Melnitchouk, and J.A. Tjon, Phys. Rev. **C72**, 034612 (2005).

[22] P. Bosted, Phys. Rev. **C51**, 409 (1995).

[23] J. Mar *et al.*, Phys. Rev. Lett. **21**, 482 (1968).

[24] J. Arrington *et al.*, *Beyond the Born Approximation: A Precise Comparison of e^+p and e^-p Elastic Scattering in CLAS*, PR04-116, PAC26 (2004)

[25] J. Arrington *et al.*, *Two photon exchange of electrons/positrons on the proton*, Proposal at VEPP-3, nucl-ex/0408020 (2004).

[26] S. Kowalski *et al.*, *Measurement of the Two-Photon Exchange Contribution in ep Elastic Scattering Using Recoil Polarization*, Jefferson Lab Proposal E04-019 (2004).

[27] D.J. Margaziotis *et al.*, *Measurement of the Target Single-Spin Asymmetry in Quasi-Elastic* $^3He^{\uparrow}$*(e,e')*, Jefferson Lab Proposal E05-15, PAC27 (2005).

[28] D. Cheever *et al.*, Nucl. Instr. Meth. **A556**, 410 (2006).

[29] C. Tschalaer, private communication.

[30] C. Altunbas *et al.*, Nucl. Instr. Meth. **A490**, 177 (2002).

[31] G. Höhler *et al.*, Nucl. Phys. **B114**, 505 (1976).